OXFORD

SOT | Society of Toxicology
www.toxsci.oxfordjournals.org

TOXICOLOGICAL SCIENCES, 150(2), 2016, 269–282

doi: 10.1093/toxsci/kfw013
Advance Access Publication Date: January 21, 2016
Research Article

PBPK-Based Probabilistic Risk Assessment for Total Chlorotriazines in Drinking Water

Charles B. Breckenridge,*[,1] Jerry L. Campbell,[†] Harvey J. Clewell,[†] Melvin E. Andersen,[†] Ciriaco Valdez-Flores,[‡] and Robert L. Sielken, Jr.[§]

*Syngenta Crop Protection, LLC, Greensboro, North Carolina, 27419-8300; [†]The Hamner Institutes for Health Sciences, 6 Davis Drive, Research Triangle Park, North Carolina, 27709; [‡]3131 Texas A&M University, College Station, Texas, 77843-3131; and [§]Sielken and Associates Consulting Inc, 1200 Beacon Court, College Station, Texas, 77845

[1]To whom correspondence should be addressed at Syngenta Crop Protection, LLC, 410 S. Swing Road, Greensboro, North Carolina 27320. Fax: 336 632 7581. E-mail: charles.breckenridge@syngenta.com.

ABSTRACT

The risk of human exposure to total chlorotriazines (TCT) in drinking water was evaluated using a physiologically based pharmacokinetic (PBPK) model. Daily TCT (atrazine, deethylatrazine, deisopropylatrazine, and diaminochlorotriazine) chemographs were constructed for 17 frequently monitored community water systems (CWSs) using linear interpolation and Krieg estimates between observed TCT values. Synthetic chemographs were created using a conservative bias factor of 3 to generate intervening peaks between measured values. Drinking water consumption records from 24-h diaries were used to calculate daily exposure. Plasma TCT concentrations were updated every 30 minutes using the PBPK model output for each simulated calendar year from 2006 to 2010. Margins of exposure (MOEs) were calculated (MOE = [Human Plasma TCT_{POD}] ÷ [Human Plasma TCT_{EXP}]) based on the toxicological point of departure (POD) and the drinking water-derived exposure to TCT. MOEs were determined based on 1, 2, 3, 4, 7, 14, 28, or 90 days of rolling average exposures and plasma TCT C_{max}, or the area under the curve (AUC). Distributions of MOE were determined and the 99.9th percentile was used for risk assessment. MOEs for all 17 CWSs were >1000 at the 99.9th percentile. The 99.9th percentile of the MOE distribution was 2.8-fold less when the 3-fold synthetic chemograph bias factor was used. MOEs were insensitive to interpolation method, the consumer's age, the water consumption database used and the duration of time over which the rolling average plasma TCT was calculated, for up to 90 days. MOEs were sensitive to factors that modified the toxicological, or hyphenated appropriately no-observed-effects level (NOEL), including rat strain, endpoint used, method of calculating the NOEL, and the pharmacokinetics of elimination, as well as the magnitude of exposure (CWS, calendar year, and use of bias factors).

Key words: atrazine; chlorotriazines; pharmacokinetics; PBPK model; drinking water; atrazine monitoring program; Safe Drinking Water Act; probabilistic risk assessment; sensitivity analysis.

Atrazine (6-chloro-N2-ethyl-N4-isopropyl-1,3,5-triazine-2,4-diamine; CAS No. 1912-24-9) is a herbicide used for preplant and early postplant control of broadleaf weeds and some grasses in corn and sorghum grown in the continental United States (Bridges, 2008). The chlorotriazines (atrazine, simazine, propazine, and terbuthylazine) continue to play an important role in weed control and the management of weed resistance in the United States, Europe (terbuthylazine), and Australia. However, because of the potential for runoff from treated fields into surface water, as well as a moderate mobility that permits the chlorotriazines to reach groundwater (Thurman and Scribner, 2008), concerns have been raised about risks associated with human exposure to this class of chemicals. Hazard profiles have been well characterized for atrazine (ATZ) and

its chlorotriazine metabolites deethylatrazine (DEA), deisopropylatrazine (DIA), and diaminochlorotriazine (DACT) (Breckenridge *et al.*, 2010). The data support the conclusion that the chlorotriazines share a common mechanism of toxicity (USEPA, 2002). Human risk was assessed in this study by estimating the cumulative exposure to total chlorotriazines (TCT) appearing in drinking water and then calculating distributions of margins of exposure (MOEs), based on sensitive toxicological points of departure (POD). Detailed evaluations of the endocrine mode of action of the triazines have been published (Cooper *et al.*, 2007; Simpkins *et al.*, 2011), and epidemiological evidence of associations between triazine exposure and various cancers and reproductive outcomes have been reviewed elsewhere (Boffetta *et al.*, 2013; Goodman *et al.*, 2014; Sathiakumar *et al.*, 2011).

The most sensitive effect of ATZ in animal studies is the suppression of the preovulatory luteinizing hormone (LH) surge in female Sprague Dawley (SD) rats administered ATZ in the diet for 6 months (Simpkins *et al.*, 2011). The no-observed-effect level (NOEL) from this study (NOEL = 1.8 mg/kg/d) has been used by the United States Environmental Protection Agency (USEPA) (2006) and the World Health Organization (WHO) (2010) to establish the POD for the chlorotriazines and to evaluate intermediate term and lifetime risks of exposure to ATZ and TCT. The USEPA concluded that using the POD based on LH surge suppression in neuroendocrinologically aged, female SD rats was conservatively protective of human health (USEPA, 2013). Shorter-duration administration of ATZ by gavage to adult female SD (Minnema, 2001), Wistar (McMullin *et al.*, 2004), or Long Evans (LE) rats (Cooper *et al.*, 2007) resulted in NOELs higher than the levels observed following chronic dietary administration (Simpkins *et al.*, 2011). Although the USEPA has officially maintained the uncertainty factor (UF) for calculating the chronic reference dose and the maximum contaminant level (MCL) for ATZ in drinking water at 1000, the WHO used a UF = 100 for calculating the acceptable daily intake of ATZ. It is likely that as new standards are set to regulate exposure to TCT, the UF will be reduced, especially if pharmacokinetic models are used to assess risk. It is generally accepted that when physiologically based pharmacokinetic (PBPK) models are used to scale rodent doses to man, there is no need to employ a 2.5- to 3-fold scaling factor that traditionally is used to extrapolate the administered dose in animals to man (Renwick and Lazarus, 1998; WHO, 2005).

Bolus dose (BD) administration of ATZ to young adult female SD rats daily for 4 days resulted in a $NOEL_{BD}$ of 10 mg/kg/d. A POD of 2.56 mg/kg/d, calculated for LH suppression in LE rat based on the 95th-percentile lower bound benchmark dose (BMDL) (Cooper *et al.*, 2010; USEPA, 2011a), was also used in this assessment. A distributed dose (DD), NOEL ($NOEL_{DD}$) of 50 mg/kg/d, also evaluated in this assessment, was from a study where ATZ was administered in the diet over 4 successive days (Foradori *et al.*, 2014). The 5-fold difference in NOELs following bolus versus DD administration is likely explained by rapid absorption and short plasma clearance half-lives of ATZ and its chlorotriazine metabolites following oral dosing. BD administration results in higher peak plasma TCT concentrations than when the dose is distributed over time. The distributed-dosing scenario more closely resembles potential human exposure to the chlorotriazines in drinking water, where the daily dose is temporally distributed over the day.

This study provides a comprehensive risk assessment for the chlorotriazines in drinking water by calculating MOEs from chemograph-based human exposure profiles and a conservative estimate of the human NOEL/POD. Exposure was determined by using TCT chemographs along with daily surveys of individual human water consumption (Barraj *et al.*, 2009). The resulting temporal pattern of human exposure was converted to estimated, time-dependent, internal human plasma TCT concentrations using a PBPK model (Campbell *et al.*, 2016). The human POD was established by using the PBPK model to convert an administered TCT-POD dose to the TCT-POD plasma concentration (Figure 1). The ratio of the model-derived human TCT concentration in plasma, at the selected POD, to the human TCT plasma resulting from exposure to TCT in drinking water was calculated for each scenario. Sensitivity analyses were conducted to evaluate the impact of changes in PBPK model parameters and risk assessment input variables, including chemographic characteristics (days within a year, season, and location), human factors (age, gender, and water consumption), selection of the NOEL/POD, water sampling frequency, and methods used to interpolate between measured TCT concentrations. Overall, the results indicate that there were acceptable MOEs for all scenarios evaluated.

MATERIALS AND METHODS

ATZ water concentration data collected under the Safe Drinking Water Act

Community water system (CWS) Safe Drinking Water Act (SDWA) compliance monitoring data were used to produce a national assessment of people potentially exposed to ATZ via drinking water. ATZ monitoring data, CWS information, and population data were collected from the leading SDWA agencies from 50 states for the years 2001 through 2009. The SDWA data were entered into a Microsoft Access database and a Population Linked Exposure program was used to determine the number of individuals who may have been exposed to ATZ or its chlorometabolites via water supplied by CWSs (Tierney *et al.*, 2008).

ATZ water monitoring program

CWSs were selected for frequent monitoring of ATZ and its metabolite residues in finished drinking water if any sample collected under the SDWA was >1.6 ppb or if the TCT concentration was >12.5 ppb (USEPA, 2004). There were 149 CWSs that met these criteria during the period from January 2006 through December 2010 (Figure 2). For each of the 149 CWSs, drinking water samples were collected weekly from approximately April 1 through July 31 and every other week during the remainder of the period from January 2006 through December 2010. Chemographs for TCT (ATZ + DEA + DIA + DACT) were constructed for each CWS; piecewise, linear interpolation was used to fill in daily values between sampling data points. The concentration on the first and last sampling date of each year was used to extend the chemograph back to January 1 and forward to December 31 for each calendar year; Supplementary Figure S2 provides a typical chemograph for one CWS.

For each CWS, interpolated daily concentrations were used to calculate 4-, 7-, 14-, 28-, and 90-day rolling averages for ATZ and TCT. All possible rolling averages of the specified duration were calculated. For example, 4-day rolling averages were calculated rolling forward starting on the first day, the second day, the third day, etc. and continuing until the end of the of the year (Supplementary Figure S2, bottom panel). Rolling average concentrations in drinking water were calculated for the purpose of regulatory compliance and were not used as inputs to the PBPK

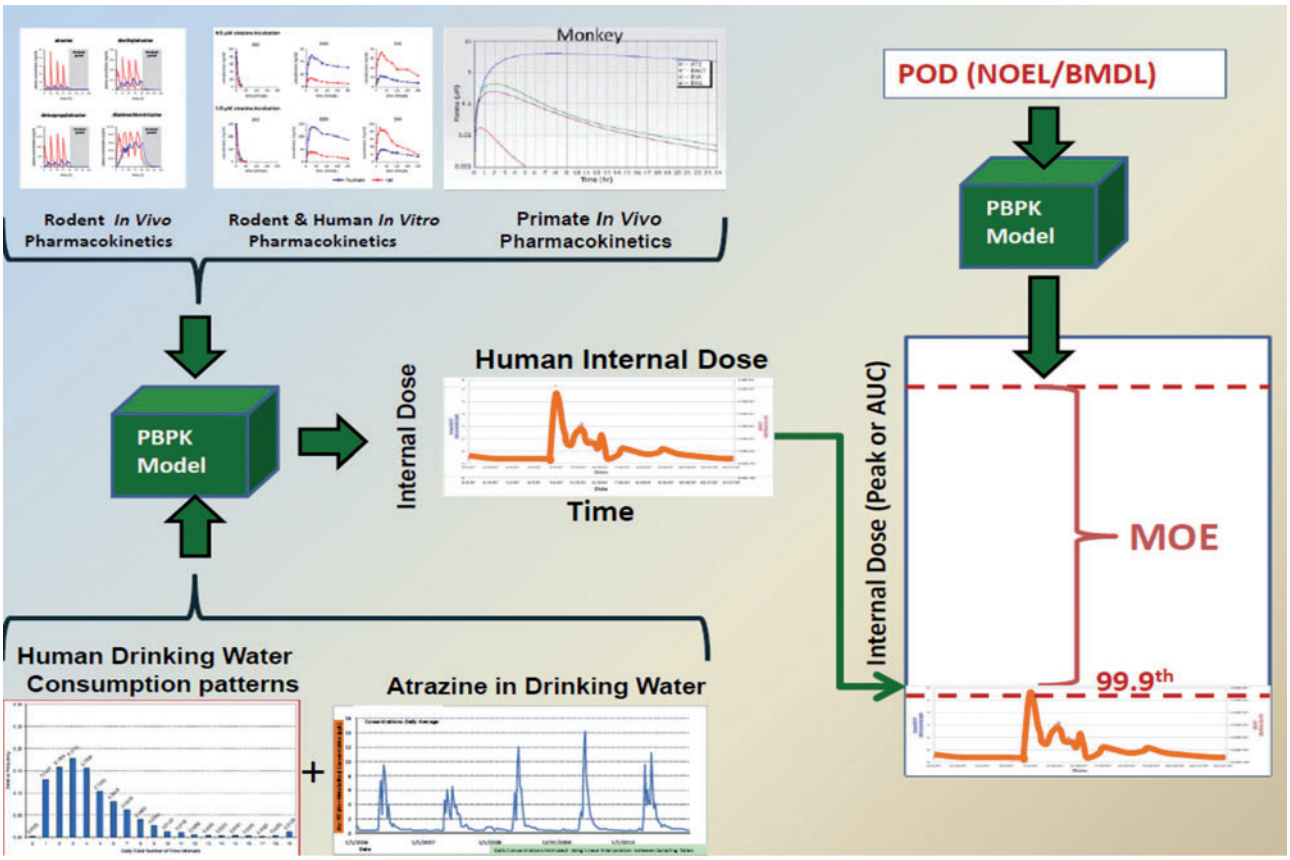

FIG. 1. Schematic representation of the use of a PBPK model to characterize human exposure (human internal dose) and risk (MOE).

model. Rolling averages of plasma TCT concentrations were calculated for risk assessment.

Estimation of TCT concentrations between weekly samples

To assess the reliability of using linear interpolation of daily TCT concentrations between weekly measurements, finished water samples were collected daily from April 1 to July 31, 2011 for 1 CWS (No. 44); biweekly samples were collected during the remainder of the year. Chemographs were constructed using either the full dataset or 7 alternate chemographs created by dropping out 6 of 7 successive daily values to reproduce the result that would have been obtained from a weekly sample on a fixed day of each week. Linear interpolation between weekly measured samples and 6 Krige-estimated intervening values were also calculated using the procedure described by Skøien and Blöschl (2007). In addition, synthetic TCT peaks were inserted between weekly concentrations. Distributions of MOEs were calculated for each of the 2 estimation procedures and compared with MOEs based on daily measurement.

Interpolation of additional TCT peaks between samples

Assuming that the weekly sampling protocol used throughout this study may have missed the occurrence of peak TCT concentration, synthetic chemographs (Supplementary Figure S3) were created for each of the 17 CWSs. An artificial TCT peak was inserted midway between each measured weekly TCT concentration. TCT concentrations between the observed and the synthetic TCT peak were linearly interpolated to produce 365-day synthetic chemographs. The synthetic chemographs for CWS No. 132 are shown for 2008 (Supplementary Figure S4) and the period from 2006 through 2010 (Supplementary Figure S5). In the middle panel of each figure, a mid-point peak was superimposed between TCT concentrations measured weekly from April to July (top panel). The concentrations represented by the synthetic data points were calculated by multiplying the higher of the 2 adjacent measured concentrations by a conservative bias factor of 3. An analysis of 4 National Center for Water Quality Research sites that included data from many seasons (Chen *et al.*, 2011) indicated a range of bias factors between 1.90 and 2.73 for converting 7-day monitoring measurements to 4-day rolling average concentrations. This value is consistent with bias factors ranging from 2 to 4 for CWSs that are monitored weekly (USEPA, 2006).

Drinking water consumption

The USDA Continuing Survey of Food Intake of Individuals (CSFII) (USDA, 2000) is used by pesticide dietary exposure models [DEEM (Exponent, 2008); Cumulative and Aggregate Risk Evaluation (CARES) (ILSI Research Foundation, 2008)] to estimate daily food and water intake. CSFII reported 24-h estimates of direct water consumption and temporally distributed estimates of daily water intake derived from the consumption of food and beverages where water was added to food during its preparation (indirect water consumption). Only the indirect water intake estimates were used in this assessment because CSFII reported the amount and the time of day that food was consumed.

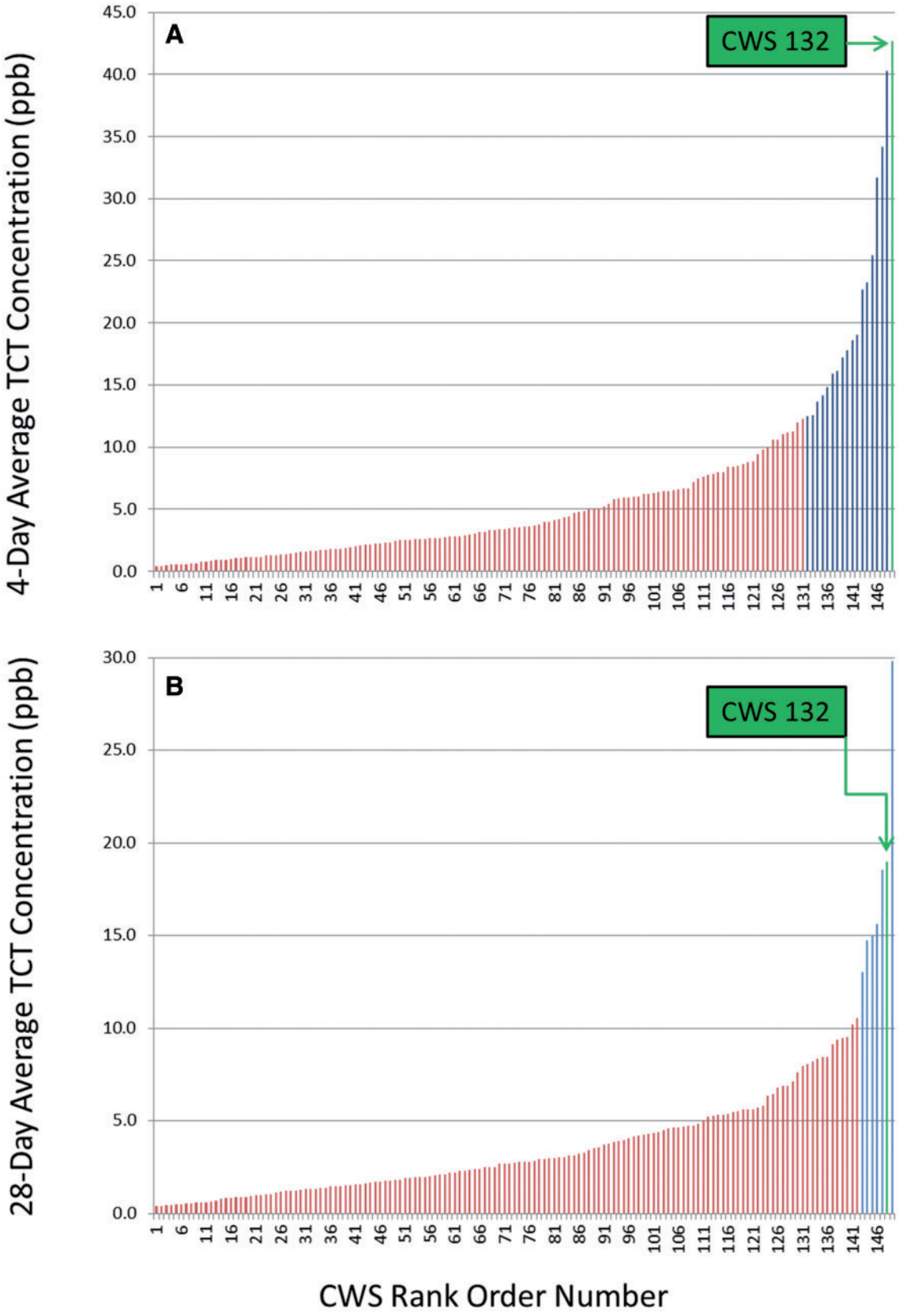

FIG. 2. Rank order of 149 CWSs in the AMP of the maximum 4-day (Panel A) and 28-day (Panel B) TCT concentrations in drinking water in any year during the monitoring period from 2006 through 2010 (CWSs designated in blue had a 4- or 28-day average concentration that exceeded 12.5 ppb).

For direct drinking water consumption (nonfood-based water), data from a nationwide drinking water consumption survey (DWCS) (Barraj *et al.*, 2009) were used because the timing and volume of direct water consumed during the day was reported. The DWCS was based on a 7-day diary of water consumption collected for 4198 individuals during the summer or winter. The number of ounces of water consumed was combined with age- and gender-specific body weight distributions from the EPA Exposure Factors Handbook (USEPA, 2011b) to calculate the number of liters of water consumed per kilogram body weight per day.

PBPK model simulation of human plasma TCT concentration

The PBPK model, described by Campbell *et al.* (2016), was used to calculate the internal plasma concentrations of TCT following exposure to ATZ, DEA, DIA, and DACT in drinking water (Figure 1). Individuals were randomly selected from the U.S. population using the CARES (ILSI Research Foundation, 2008). Individual water consumption and body weight data were paired with the daily concentrations of ATZ and its chlorometabolites, as represented by the chemograph for a randomly selected CWS. These concentrations, which were updated every 30 min, were converted by the PBPK model into plasma TCT concentrations. Peak plasma TCT concentration (μmol/l) and TCT-AUC (μmol×h/l) calculated over the averaging period were used because these dose metrics are plausibly related to the effect of ATZ on LH (Simpkins *et al.*, 2011).

Points of departure

PODs were based upon NOELs or the 95th percentile Redundant. BMDL for the effect of ATZ on the LH surge in SD (Foradori *et al.*, 2014) or LE rats (Cooper *et al.*, 2010; Foradori *et al.* 2014) administered ATZ either as a BD by gavage or as a temporally DD in animal feed. The NOELs were as follows: $NOEL_{BD}$ = 10 mg/kg/d (Foradori *et al.*, 2014); $NOEL_{DD}$ = 50 mg/kg/d (Foradori *et al.*, 2014); and $BMDL_{BD}$ = 2.56 mg/kg/d (Cooper *et al.*, 2010; USEPA, 2011a).

These PODs were selected because they were the most sensitive to the effect of short-duration (ie, 4 days) exposure of animals to ATZ. The DD NOEL of 50 mg/kg/d was included in this assessment because DD administration is considered to better reflect the temporal pattern of human exposure to ATZ and its chlorometabolites in drinking water than BD administration. The PODs used in all sensitivity analyses were based upon the $NOEL_{BD}$ = 10 mg/kg/day derived from the effect of a BD of ATZ on the LH surge in the female SD rat (Foradori *et al.*, 2014). This NOEL was selected because the resulting distributions of MOEs could be easily scaled to any NOEL or POD, including the NOEL of 1.8 mg/kg/d currently utilized by regulatory authorities to evaluate the risk of lifetime exposure to ATZ (USEPA, 2006; WHO, 2010).

Margins of exposure

The MOE was calculated as the ratio of the TCT_{Peak} (or TCT_{AUC}), model-derived plasma concentration in humans exposed to TCT in drinking water (DW dose) to the plasma concentration in humans at the POD dose as follows:

$$\text{MOE} = \frac{\text{Human peak plasma TCT concentration at the POD}}{\text{Human peak plasma TCT concentration at DW dose}}$$

In the baseline risk characterization case (ie, POD = 10 mg/kg/d), MOEs were calculated by randomly matching individual drinking water consumption values to each consecutive 4-day TCT concentration in the worst-case calendar year for a CWS. For each drinking water consumption year simulated, the 365-day profile of drinking water consumption for an individual was used for the worst-case calendar year and the randomly selected CWS. In the baseline risk characterization case, 28 drinking water consumption years were simulated (362, 4-day rolling averages per year × 28 years = 10 136, 4-day rolling averages). In alternative scenarios using different PODs, 100 drinking water consumption years were simulated, corresponding to 100 individuals for each CWS evaluated (362, 4-day rolling averages per year × 100 years = 36 200, 4-day rolling averages). For each set of simulations, a distribution of the MOEs was plotted (Supplementary Figure S6) and the MOE at the 99.9th percentile was tabulated.

Sensitivity analyses

This study used the PBPK model described by Campbell *et al.* (2016) to predict plasma concentrations of ATZ, DEA, DIA, and DACT in simulated humans exposed to the chlorotriazines in drinking water. These plasma concentrations depend on both the model structure and the values assigned to a number of physiological parameters and rate constants associated with the absorption, distribution, metabolism, and clearance of the chlorometabolites. The effect of model parameter value selection on model output was assessed by calculating the MOE for an approximately 70 kg person exposed to chlorotriazines in drinking water (CWS No. 44 sampled weekly or biweekly in 2009) based on the standard 'fixed parameter' model (POD = 10 mg/kg/d BD, TCT_{AUC}, 4-day rolling average). The base-case MOEs were calculated using the 84 model parameter values specified in Supplementary Tables S1 and S2. The random-case distributions of MOEs were obtained by randomly selecting each of the 84 model parameters from either a normal or log-normal distribution that had coefficients of variation equal to 0.5 or 50%, respectively. Two drinking water intake scenarios were evaluated for CWS No. 44 in 2009. These scenarios corresponded to risks associated with water intake of 2 hypothetical individuals who were at the 95th (MOE = 58 928) or 99.9th (MOE = 13 047) percentiles of the base-case MOE distribution. For each scenario, the mean and median MOEs were calculated from the 362, 4-day rolling average TCT AUCs. For each model simulation, a coefficient of determination was calculated for each of the 84 model parameters to determine which model parameter(s) accounted for the greatest amount of variation in the distribution of MOEs.

The effect of model inputs on PBPK model outputs (TCT_{Peak} and TCT_{AUC}) was also evaluated using Monte Carlo simulation. Input variables that were assessed included differences in (1) POD and plasma pharmacokinetic parameters (TCT_{Peak}, TCT_{AUC}); (2) rolling average durations; (3) chemographic characteristics (CWS, year); (4) personal characteristics (age, gender, water intake); and (5) data interpolation or simulation methodologies (Supplementary Table S3).

RESULTS

Safe Drinking Water Act Compliance Monitoring Data (2001–2009)

In December 2009, there were 49 288 CWSs in the United States (Table 1), excluding CWSs serving tribal territories, U.S. territories and the District of Columbia. There were 38 631

TABLE 1. SDWA ATZ Compliance Monitoring Program in continental United States CWSs from 2001 through 2009 and the estimated populations served by these CWSs

	Grand Total		Ground Water		Surface Water		Other	
	Total	Percent	Total	Percent	Total	Percent	Total	Percent
Samples[a]	142 545		99 208		29 993		13 344	
Nondetections	133 323	(93.53%)	97 344	(98.12%)	24 342	(81.16%)	11 637	(87.21%)
Detections	9222	(6.47%)	1864	(1.88%)	5651	(18.84%)	1707	(12.79%)
Detections > 3.0 ppb	266	(0.19%)	11	(0.01%)	229	(0.76%)	26	(0.19%)
Minimum-detected concentration (ppb)	0.01		0.01		0.01		0.05	
Maximum detected concentration (ppb)	40		14		40		13	
99.9th-percentile concentration (ppb)	4.49		1.50		10.60		4.40	
CWS[a]	49 288		38 631		9434		1223	
CWS with ATZ data	31 426	(63.76%)	24 326	(62.97%)	5893	(62.47%)	1207	(98.69%)
CWS with monitoring waiver	16 733	(33.95%)	13 483	(34.90%)	3235	(34.29%)	15	(1.23%)
CWS with data or waiver	48 159	(97.71%)	37 809	(97.87%)	9128	(96.76%)	1222	(99.92%)
CWS without data or waiver	1129	(2.29%)	822	(2.13%)	306	(3.24%)	1	(0.08%)
CWS with no detections[a]	29 094	(92.58%)	23 848	(98.04%)	4222	(71.64%)	1024	(84.84%)
CWS with detections	2332	(7.42%)	478	(1.96%)	1671	(28.36%)	183	(15.16%)
CWS with detections > 3.0 ppb	272	(0.87%)	9	(0.04%)	245	(4.16%)	18	(1.49%)
CWS with annual means > 3.0 ppb	21	(0.07%)	1	(0.004%)	19	(0.32%)	1	(0.08%)
CWS with period means > 3.0 ppb	0	(0.00%)	0	(0.00%)	0	(0.00%)	0	(0.00%)
50 State population[a]	308 143 815							
Population on CWS	283 675 933	(72.07%)	96 736 914	(23.98%)	151 581 347	(36.69%)	35 357 672	(11.40%)
Population served by CWS with data	222 081 906	(78.29%)	73 893 314	(76.39%)	113 071 910	(74.59%)	35 116 682	(99.32%)
Population served by CWS with monitoring waiver	60 084 090	(21.18%)	22 627 366	(23.39%)	37 215 894	(24.55%)	240 830	(0.68%)
Population served by CWS with data or waiver	282 165 996	(99.47%)	96 520 680	(99.78%)	150 287 804	(99.14%)	35 357 512	(100.00%)
Population Served by CWS without Data or Waiver	1 509 937	(0.53%)	216 234	(0.22%)	1 293 543	(0.85%)	160	(0.00%)
Population with no detections[b]	176 079 260	(79.29%)	68 934 370	(93.29%)	80 418 672	(71.12%)	26 726 218	(76.11%)
Population with detections	46 002 646	(20.71%)	4 958 944	(6.71%)	32 653 238	(28.88%)	8 390 464	(23.89%)
Population with detections > 3.0 ppb	4 262 600	(1.92%)	16 255	(0.02%)	1 561 903	(1.38%)	2 684 442	(7.64%)
Populations with annual means > 3.0 ppb	84 686	(0.04%)	2410	(0.003%)	68 276	(0.06%)	14 000	(0.04%)
Populations with period means > 3.0 ppb	0	(0.00%)	0	(0.00%)	0	(0.00%)	0	(0.00%)

[a]Percent of samples, CWSs, and populations with or without detects are based on the number of assessed samples, CWSs, and populations, respectively.
[b]Percent of CWSs.

groundwater-supplied, 9434 surface-water-supplied. and 1223 other-water-sources-supplied CWSs (Table 1). The corresponding populations served were 96.7 million on groundwater, 151.6 million on surface water, and 35.4 million individuals supplied with drinking water from other sources (Table 1).

In the United States, an estimated total of 283.7 million people were provided drinking water by CWSs (Table 1). CWSs with no ATZ detects from 2001 to 2009 provided finished drinking water to 176 million people. An additional 60 million people were supplied by CWSs that that waived out of the requirement for ATZ monitoring under the SWDA, generally because of an absence of detections earlier in the program. CWSs that had ATZ detects in one or more samples during the period from 2001 through 2009 period supplied 46.0 million people.

Twelve CWSs had one or more ATZ annual mean concentrations of greater than the MCL of 3 parts per billion (ppb). Two of the 12 CWSs provided drinking water to 9 additional CWSs which did not produce their own finished water. Taken together, these 21 CWSs served a combined population of approximately 84 686 people. The 21 CWSs identified by SDWA were also in the ATZ monitoring program (AMP) or the Syngenta voluntary monitoring program.

AMPs (2006–2010)

Seventeen of the 149 CWSs monitored frequently in the AMP programs had 4-day average TCT concentrations that exceeded the EPA standard of 12.5 ppb for a least one 4-day period during the interval from 2006 to 2010 (Figure 2 panel A). Seven of these 149 CWSs had at least one 28-day rolling average exceeding 12.5 ppb (Figure 2 panel B). Fourteen of the 149 CWS in the AMP had at least one year where the 4-quarter, annualized mean ATZ concentration was greater than the MCL during the period from 2001 through 2009. These 14 CWSs were among the 17 CWSs that were selected for more detailed analyses.

Chemographs for the CWS (No. 132) with the greatest 4- and 28-day rolling averages are displayed in Supplementary Figure S2. Measured TCT concentrations (Panel A), TCT concentrations linearly interpolated between measured concentrations (Panel B), and 4-day, rolling-average concentrations (Panel C) are presented. The calculated 4-day, rolling-average TCT concentrations for CWS No. 132 in 2008 (blue line) are compared to the PBPK-calculated 4-day, rolling-average plasma TCT AUC (red line), as shown in Figure 3. The PBPK-model-derived 4-day, rolling-average plasma TCT concentration scaled perfectly to the calculated, 4-day, rolling-average TCT concentration in drinking water.

The chemograph for CWS No. 44 for the years from 2006 through 2011 (Figure 4a) was comprised of the standard weekly/biweekly samples from 2006 through 2010, and daily water samples collected from April 1 through July 31 in 2011. The TCT peak concentration during the critical runoff period was greatest in 2011 when samples were collected daily, as opposed to the weekly samples taken in preceding years.

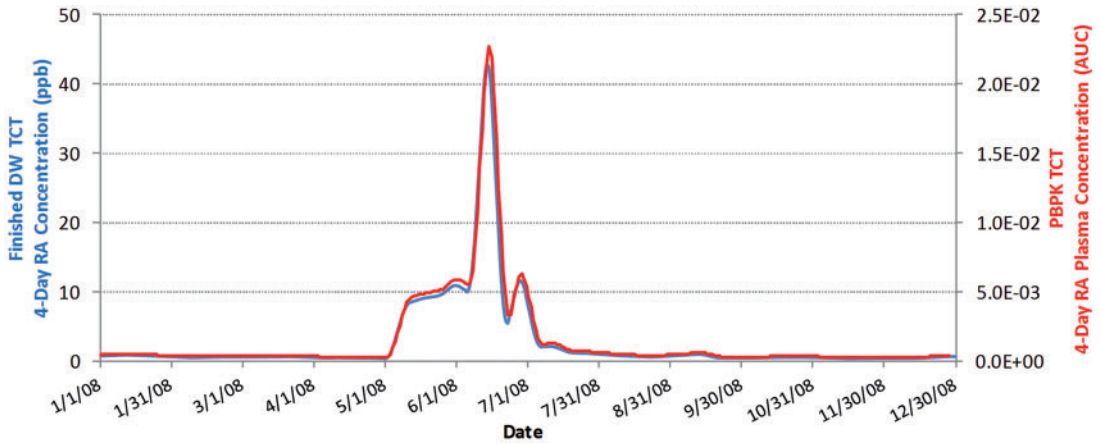

FIG. 3. Comparison of the 4-day, rolling-average concentration in finished drinking water for CWS No. 132 (blue) to the PBPK-predicted plasma concentration AUC scaled to an internal dose (as $\mu g \times ml^{-1} \times h^{-1}$), following simulated daily ingestion of water from the CWSs.

Krige-estimated TCT and comparable linear-interpolated TCT concentrations, assuming that samples were taken on days 5, 12, 19, etc. from April 1 to July 31 in 2011 are compared with daily-measured TCT concentrations (Figure 4b; see Supplementary Figure S10 for the entire series of 6 Krige-estimated TCT concentations). The results indicate that Krige-estimated values were no more reliable than linear-interpolated estimates for systems that display rapidly fluctuating TCT concentrations. Depending on the timing of sample collections with respect to randomly occurring runoff events, both methods failed to detect peak concentrations of rapidly occurring runoff events. In Figure 4b, based on samples drawn weekly and commencing on April 5 (K5 estimate), both methods failed to detect small amplitude runoff events that occurred on May 11, May 25, and June 15, yet they accurately characterized the large-amplitude event that occurred on June 23. In contrast, when water sampling commenced on the K6 or K7 intervals, the small runoff events were well described, but the major runoff event that occurred on June 23 was underestimated by approximately 2.5-fold (Supplementary Figure S10).

Margins of Exposure

The 99.9th percentiles of the distribution of MOEs were all above 1000 for each measure of internal dose (TCT peak or AUC) and POD (BD vs. DD), irrespective of the exposure level in the 17 vulnerable CWSs selected for probabilistic risk assessment using the PBPK model (Figure 5). The cumulative probability density distribution for CWS No. 132, the highest-ranking, worst-case CWS of the 149 CWSs in the AMP, is shown in Supplementary Figure S6.

CWS location and the year in which water samples were collected had the largest impacts on MOE magnitude (Figure 6, top panel). For the 17 most vulnerable CWSs in the program, the largest 99.9th-percentile MOE (MOE_{Max} = 200 532) calculated over the 5-year monitoring program was approximately 49-fold greater (CWS No. 96) than the smallest MOE (MOE_{Min} = 4059) observed in the same CWS (Table 2, Row 3). Year-to-year variability contributed significantly to this difference. For example, the largest MOE observed for CWS No. 96 was observed in 2008 and the smallest MOE was seen 2 years later in 2010 (Figure 6; Table 2).

Sensitivity Analyses

The selection of the POD reduced the MOEs observed at the 99.9th percentile in direct proportion to the magnitude of the reduction in the POD (Figure 5; Table 2, Row 1); 99.9th-percentile MOEs based on peak plasma TCT concentrations were 1.46-fold greater than MOEs based upon the AUC (Figure 5; Table 2, Row 2). Age of the assessment group (13–19 years vs. 19–49 years) had a minimal effect on the 99.9th-percentile MOEs (Ratio = 1.15, Supplementary Figure S6; Table 2, Row 8).

Differences between MOEs based on 4-day rolling averages versus 28-day rolling averages were slight (Ratio = 1.09; Figure 6B; Table 2, Row 9). Larger differences between 99.9th-percentile MOEs were noted when MOEs were calculated on the basis of 28-day rolling averages vs. those calculated on the basis of 90-day rolling averages (Ratio = 2.02, Figure 5; Table 2, Row 10). MOEs calculated on consecutive 4-day rolling averages were 2.28-fold greater than those based on randomly-drawn, 4-day rolling averages (Table 2, Row 11).

Other methodological choices also influenced the 99.9th-percentile MOEs. The choice of water intake estimates (CSFII vs. Barraj [2009] direct water consumption estimates) resulted in a 2.05-fold difference in the 99.9th-percentile MOE estimates (Supplementary Figure S5; Table 2, Row 6). The use of indirect and direct water consumption versus direct water consumption alone resulted in a 1.36-fold difference in the 99.9th-percentile MOEs (Table 2, Row 7).

The effect of randomly selecting each of the 84 PBPK model parameters, compared with using the base-case, fixed set of model parameters, was assessed at both the 95th and 99.9th percentiles of the MOE distribution for CWS No. 44 in 2009 (Figure 4a). A plot featuring the distribution of the ratios of random-case MOEs to the base-case MOE is presented in Supplementary Figure S8 and the distributions for 0.1, 50, and 99.9th percentiles are provided in Table 3. The results indicate that at the median of the distribution of ratios, the random-case MOE is approximately identical to the base-case MOE (Table 2, Row 13). However, at the 0.1th percentile of the distribution of ratios, the random-case MOE was approximately one-third of the base-case MOE (Table 2, Row 12), and at the 99.9th percentile, the random-case MOE was approximately 2.4 times greater than the base-case MOE (Table 2, Row 14). Of the 84 model parameters randomly selected in each of the 1000 iterations, 99% of the

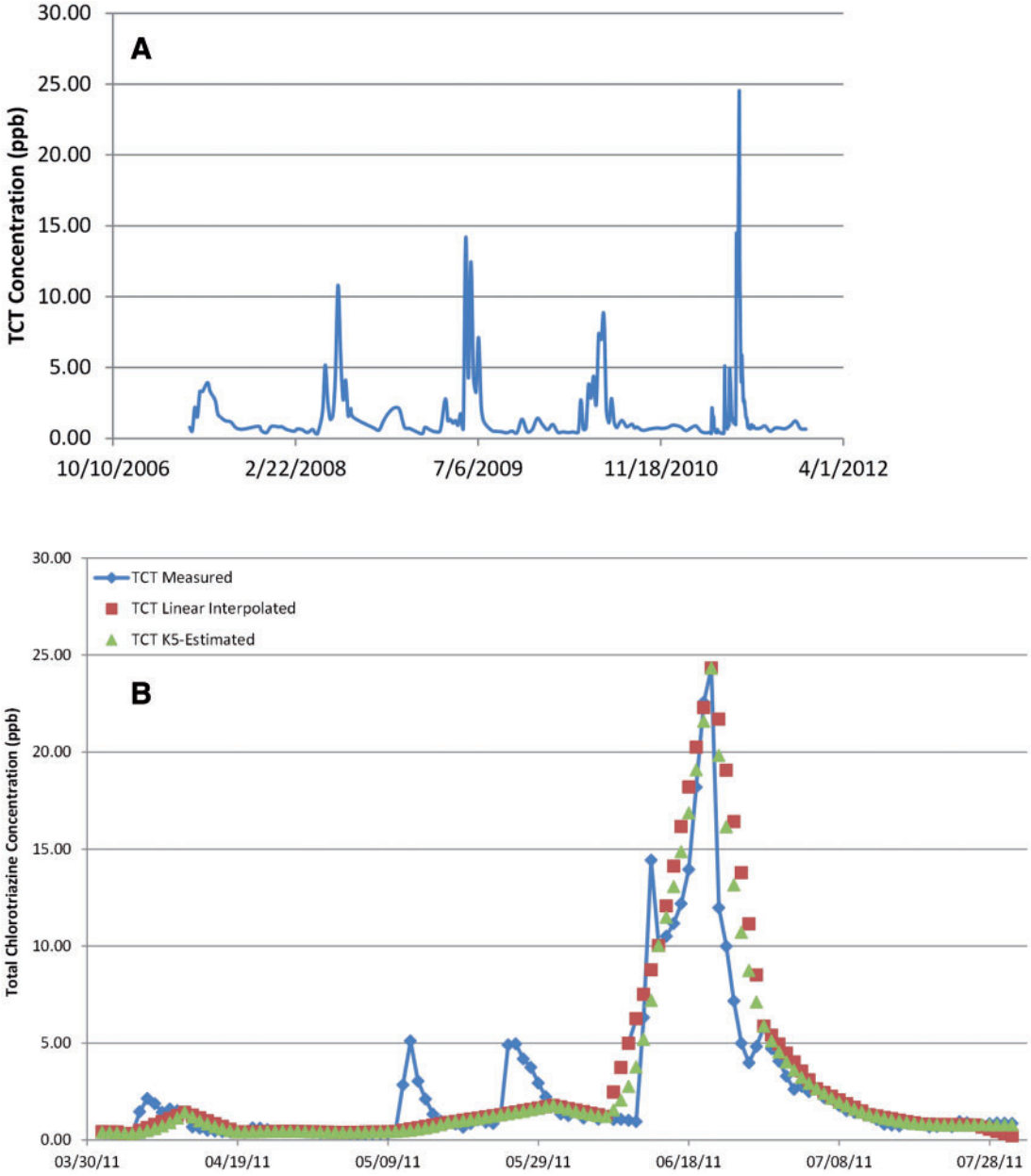

FIG. 4. A, TCT chemographs for CWS No. 44 based on weekly measured TCT concentrations in CWS No. 44 from April 1 to July 31 in the years 2007 through 2010, with daily measurements during the same interval in 2011, as well as bi-weekly measurements taken at other times of the year. **B**, TCT chemographs for CWS No. 44 based on daily-measured TCT concentrations in CWS No. 44 from April 1 to July 31 in 2011 (blue), as well as weekly measured TCT concentrations. Krieg-interpolated values are inserted between measured values (red), and weekly measured TCT concentrations with linear interpolated values are inserted between measured values (green).

between-iteration variability (ie, the coefficient of determination or $r^2 = 0.99$) was due to one model parameter, CLRDAC, the rate of urinary clearance constant for DACT. The coefficients of determination for all other 83 model parameters were <0.01.

Effect of Sample Frequency on the Estimated Daily TCT Concentration

The use of a 3-fold bias factor and the insertion of synthetic TCT peaks between measured peaks in the chemographs for the 17 CWSs (Figure 7) resulted in the maximum 99.9th-percentile MOE being reduced by a factor of approximately 2.8 (Table 2, Row 5). MOEs for the $NOEL_{BD}$ were >1700. When the amplified synthetic chemographs were assessed using EPA's proposed $BMDL_{BD}$ (2.56 mg/kg/d), the MOEs all exceeded 400.

The 99.9th-percentile MOEs for CWS No. 44 in 2011 (Table 4, K1 estimate) was based on daily-measured TCT concentrations from April 1 to July 31. For CWS No. 44, 7 alternate chemographs were constructed for the period from April 1 to July 31, 2011, by dropping out 6 intervening measured values and filling in the missing values using linear interpolation or Kriging. The 99.9th-percentile MOEs were calculated for each alternative sampling strategy based on TCT peak or AUC and a BMDL of 10 mg/kg/d. Using linear interpolation to replace missing values, the 99.9th-percentile MOEs ranged from 12 597 (K4 sample) to 27 882 (K2 sample) based on TCT peak and 8497 (K5 sample) to 16 334 (K1 sample) based on TCT AUC (Table 4). The corresponding values based on Krige-estimated

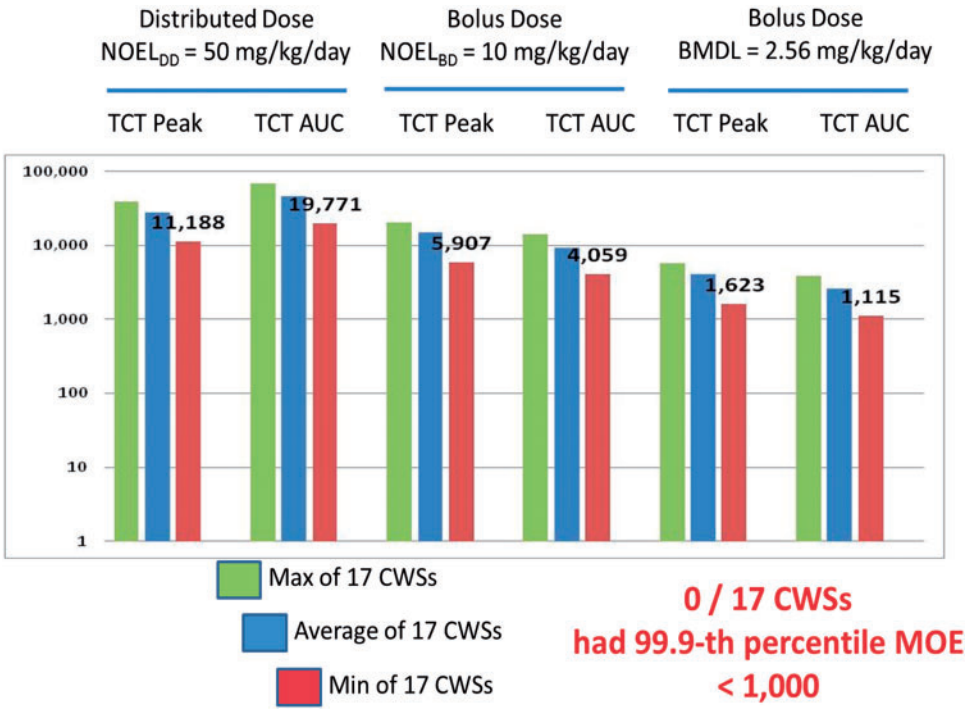

FIG. 5. Maximum, mean, and minimum MOEs at the 99.9th percentile of the distribution of MOEs for 17 CWSs calculated for the years from 2006 through 2010. MOEs were calculated as the ratio of the TCT peak or TCT AUC plasma concentrations at the POD to TCT concentrations that humans were exposed to in drinking water.

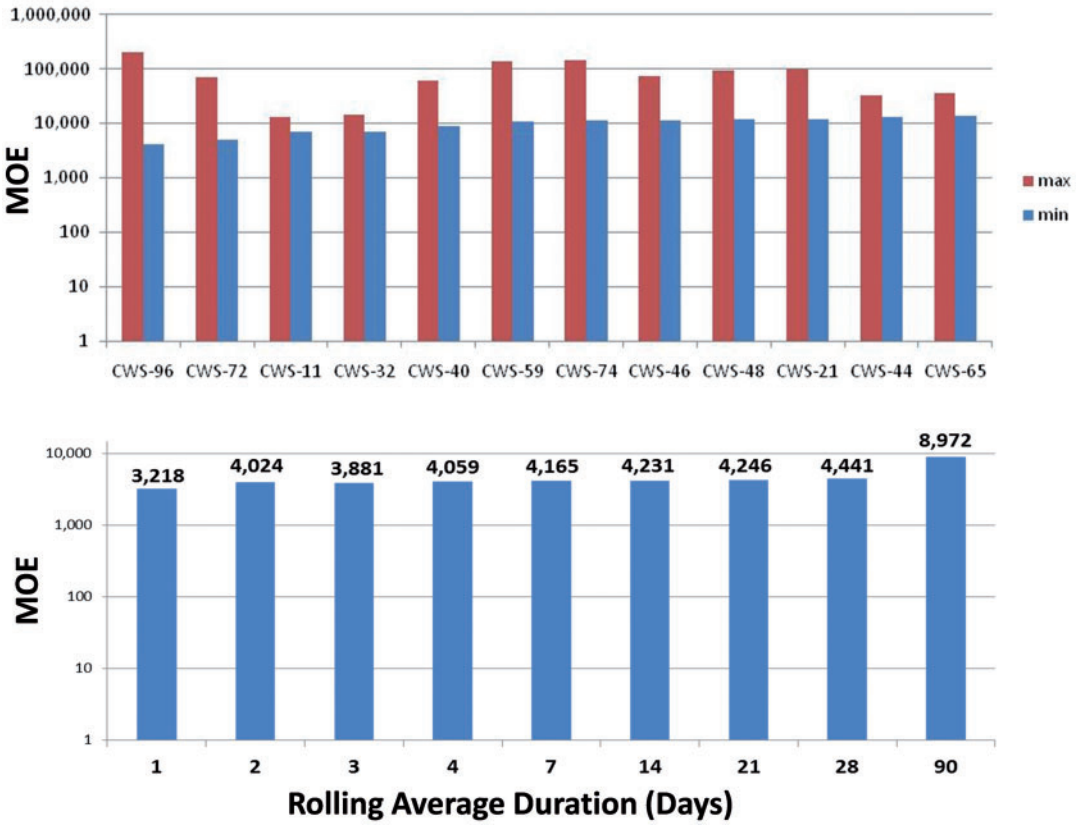

FIG. 6. Effect of the CWS location (top), or the number of days over which the rolling average TCT concentration was calculated (bottom) on the magnitude of the MOE at the 99.9th percentile of the MOE distribution.

TABLE 2. Comparison of the effect on the MOE observed at the 99th percentile of the simulated distribution of MOEs using 2 different methods or databases in the calculation

Row	Source of Data for MOE Calculation	A	B	A ÷ B
1	MOE with POD based on a DD (A) versus a BD (B)	19 771	4059	4.87
2	MOE based on TCT peak (A) versus TCT AUC (B)	5907	4059	1.46
3	Largest MOE (A) versus smallest MOE (B): CWS96	200 532	4059	49.4
4	Year (2008) with the largest MOE (A) versus the year (2010) with the smallest MOE (B): CWS 96	200 532	4059	49.4
5	MOE calculated based using linear interpolation (A) versus MOE calculated with synthetic peaks (B)	4800	1705	2.82
6	MOE based upon CSFII direct water (A) versus Barraj (2009) direct water (B)	8313	4059	2.05
7	MOE based upon CSFII direct water (A) versus direct + indirect water (B)	8313	6098	1.36
8	MOE for ages 13 to 19 years (A) versus 19 to 49 years (B)	4059	3533	1.15
9	MOE based on the 28-day (A) versus 4-day (B) rolling average: CWS96	4441	4059	1.09
10	MOE based on the 90-day (A) versus 28-day (B) rolling average: CWS96	8972	4441	2.02
11	MOE based on 4-day consecutive rolling averages in a calendar year (A) versus randomly-drawn 4-day rolling averages from 2006 to 2010 (B)	4059	1782	2.28
12	MOE based on randomly-selected model parameters (A) versus MOE based on the base-case model parameterization (B); 0.1th percentile, 99.9th drinking water intake scenario	4553[a]	13 047[b]	0.349
13	MOE based on randomly-selected model parameters (A) versus MOE based on the base-case model parameterization (B); 50th percentile, 99.9th percentile percentile drinking water intake scenario	12,616[b]	13 047[a]	0.967
14	MOE based on randomly-selected model parameters (A) versus MOE based on the base-case model parameterization (B); 99.9th percentile percentile, 99.9th drinking water intake scenario	30 804[b]	13 047[a]	2.361

[a]99.9th percentile, base-case MOE calculated for CWS No. 44 in 2009 based on TCT AUC 4-day rolling averages.
[b]The MOE at 0.1, 50, and 99.9th percentile was calculated as the product of the base-case MOE and ratio of the random-case MOE to the base-case MOE.

TABLE 3. The 0.1, 50, and 99.9th percentiles of the ratio (± SEM[b]) of the random-case median MOE[c] to the base-case MOE[d] for CWS No. 44 in 2009[e] at the 99.9th percentile drinking water intake scenario

Percentile of the distribution of the ratios	Ratio= random-case median MOE ÷ base-case MOE[f] Median ratio (± SEM)
0.1th	0.347 (± 0.039)
50th	0.967 (± 0.039)
99.9th	2.382 (± 0.039)

[a]Ratios of MOEs = random-case median MOE at the n^{th} percentile ÷ base-case MOE.
[b]SEM = standard error of the mean of 1000 iterations of the Monte Carlo simulation.
[c]Random-case median MOE = median 4-day rolling average AUC_{TCT} in the i^{th} simulation of the PBPK model parameter values ÷ POD[6].
[d]Base-case MOE = AUC_{TCT} ÷ POD; the base-case PBPK model parameter values are given in Supplementary Tables S1 and S2.
[e]362, 4-day rolling averages were calculated for TCT AUCs for each of the 1000 Monte Carlo iterations. For each rolling average, a MOE was calculated.
[f]Base-case POD for the TCT AUC = 232 μM-h/l (NOAEL = 10 mg/kg/d BD).

missing concentrations ranged from 14 334 (K4 sample) to 31 337 (K2 sample) for TCT peak and from 9300 (K5 samples) to 18 599 (K1 sample) for TCT AUC. Overall, the linear interpolation method was 9–12% more conservative (ie, smaller MOEs) than Krige-estimated MOEs. MOEs based on TCT AUC were 36% more conservative than those calculated using TCT peak. The 99.9th-percentile MOEs for CWS No. 44 from 2006 to 2009 were 10 389 and 15 049 based on TCT peak and TCT AUC, respectively ($NOEL_{BD}$ = 10 mg/kg), when TCT concentrations between weekly measured concentrations from April 1 to July 31 were estimated using linear interpolation.

DISCUSSION

This study has utilized new toxicity data (Foradori *et al.*, 2014), pharmacokinetic modeling information (Campbell *et al.*, 2016) and exposure data to conduct a high-tiered risk assessment of exposure ATZ and its chlorometabolites in frequently monitored CWSs located in continental United States (Tierney *et al.*, 2008). This study is important because it provides a unique and comprehensive quantitative characterization of exposure and risk, based on modeling and Monte Carlo simulation of the internal human dose of TCT resulting from drinking water contaminated with the chlorotriazines. The results show that MOEs >1000, the current regulatory standard utilized by the USEPA to assess ATZ risk, were observed at the 99.9th percentile of the risk distribution for the 17 CWSs, with the greatest 4- and 28-day rolling model-derived average plasma TCT concentrations found in 149 vulnerable CWSs.

The ratio of the maximum to the minimum MOEs observed at the 99.9th percentile of the risk distribution was highly sensitive to the calendar year in which the runoff event occurred. This result is consistent with the observation that runoff of ATZ is maximized if rainfall events occur shortly after application of the herbicide (Thurman and Scribner, 2008). The insertion of 3-fold synthetic TCT peaks between measured peaks in the chemographs for the 17 CWSs, a procedure that provided a worst-case estimate of TCT concentration uncertainty associated with the intermittent-sampling protocol, resulted in the 99.9th-percentile MOE being reduced by a factor of approximately 2.8. Even under these conditions, MOEs were still >1000. To verify whether the literature-based bias factor was supported by daily monitoring data from one CWS (No. 44), we computed 7 weekly TCT distributions using linear interpolation or Kriging. The maximum 99.9th-percentile MOEs were 2.2-fold greater than the

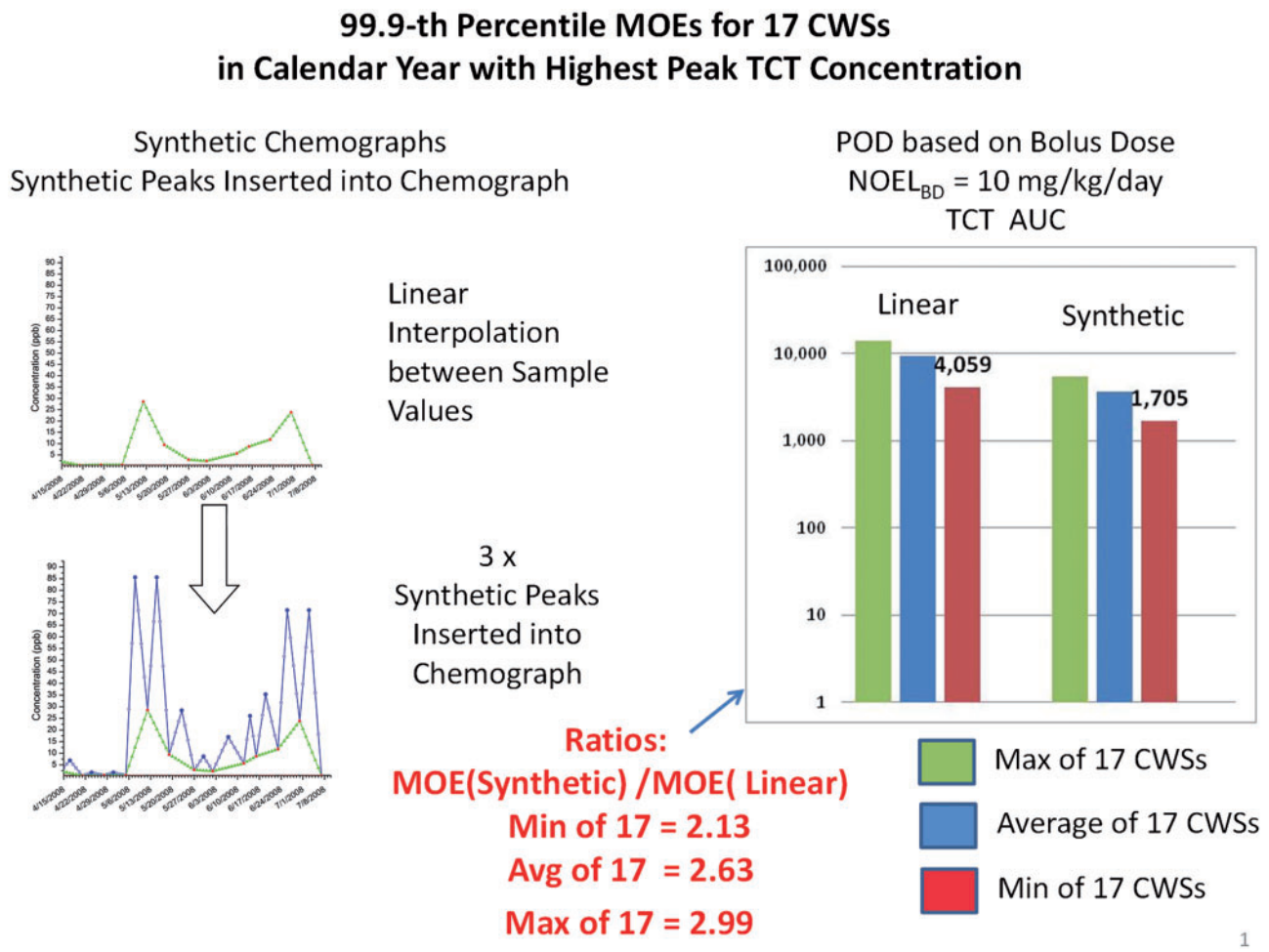

FIG. 7. Average maximum 99.9th-percentile MOEs for 17 CWSs for which the TCT concentration in water was estimated using linear interpolation between sample values or by inserting a peak that was 3-fold greater than the sample value.

Table 4. MOEs calculated using piecewise linear interpolation or Kriging to fill in missing TCT concentrations between weekly measured concentrations

Day of first weekly water sample	MOE[a]			
	TCT peak		TCT AUC	
	Linear	Kriging	Linear	Kriging
K1 (April 1)	24 439	25 657	16 334	18 599
K2 (April 2)	27 882	31 337	15 506	18 305
K3 (April 3)	20 450	20 981	11 521	12 562
K4 (April 4)	12 597	14 334	8857	9502
K5 (April 5)	14 358	15 875	8497	9300
K6 (April 6)	19 387	21 617	13 210	14 978
K7 (April 7)	20 526	23 413	14 042	16 406
Mean of K1–K7	**19 948**	**21 888**	**12 567**	**14 236**

[a] $\mathrm{MOE} = \frac{\text{Plasma } [\mathrm{TCT}]_{\text{Human NOEL–10 mg/kg/d}}}{\text{Plasma } [\mathrm{TCT}]_{\text{Human@ 99.9th percentile drinking water exposure}}}$.

minimum 99.9th-percentile MOEs based on TCT peak and 1.9- to 2-fold greater based on TCT AUC. For this CWS, Krige-estimated missing values in samples drawn every 7 days were 40% less conservative than when linear interpolation was used.

Another factor that had a large impact on the MOE was whether ATZ was administered as a bolus dose or as a temporally distributed dose. Foradori *et al.* (2014) showed that ATZ had no effect on the most sensitive toxicological outcome (ie, LH surge suppression) when ATZ was administered at the highest dose tested (roughly 50 mg/kg/d) as a distributed dose in feed (500 ppm) to SD rats. In contrast, the NOEL following bolus dosing was 10 mg/kg/d; the lowest-observed-effect level was 25 mg/kg/d. Thus, when all other factors were held constant, MOEs were roughly 5-fold greater following temporally distributed dosing compared with bolus dosing. The difference between bolus and distributed dosing may be even larger than a factor of 5 because Foradori *et al.* (2014) did not establish an effect level in the dietary study. This is important because human exposure to ATZ and its chlorometabolites in drinking water is always temporally distributed over the day, as indicated by the water intake data in CSFII and in the survey reported by Barraj *et al.* (2009). Sensitivity analyses also indicated that estimates of water intake obtained using the survey conducted by Barraj *et al.* (2009) resulted in a mean 99.9th-percentile MOE (4059) that was lower than the mean 99.9th-percentile MOE that was calculated based on direct water intake reported in CSFII (MOE = 8313) and direct plus indirect water consumption (ie, water associated with cooking food), also reported in CSFII (MOE = 6098). Hence the analysis reported as the base-case using the survey by Barraj *et al.* (2009) likely underestimated the 99.9th-percentile MOEs.

MOEs were relatively insensitive to the respective periods over which the rolling TCT plasma concentration averages were

calculated. This suggests that maximum runoff is closely coupled to the timing of application. For example, in the state of Illinois from 2001 through 2009, the average duration of time from commencement to completion of corn planting was approximately 7–8 weeks (Supplementary Figure S1). Thus, the duration of time for significant ATZ runoff into surface water was limited by the rate of corn planting, which in turn defined the window of time in the watershed when pre- and early postemergence herbicide applications occurred. In a given year, the timing of corn planting is temperature-dependent, and for a given field, runoff potential is heavily dependent on rainfall intensity and the timing of rain events with respect to planting (Thurman and Scribner, 2008). In this study, the timing and occurrence of these events was captured in the chemographs of frequently monitored CWSs.

Sensitivity analyses of other factors revealed that MOEs calculated based on TCT peak levels were 1.5-fold greater than those based upon TCT AUC measures. Biologically, it is difficult to ascertain with confidence which of these dose metrics is most appropriate for the response being evaluated. For the effect of ATZ on ACTH-dependent corticosterone and progesterone release from the adrenal gland (Fraites *et al.*, 2009; Laws *et al.*, 2009), it is likely that the peak plasma level of ATZ is the critical factor, since the maximal response appears to be triggered within 15 min by a threshold plasma concentration of ATZ. DEA and DIA are less effective, and DACT is inactive (Laws *et al.*, 2009). However, for the effect of ATZ on the LH surge, it is likely that the TCT AUC is the driving factor, because a minimum of 4 daily gavage doses of ATZ are necessary to elicit an significant reduction of the LH surge in ovariectomized SD rats (Goldman *et al.*, 2013); the effect of ATZ on the LH surge disappeared within 4 days after the last dose (Foradori *et al.*, 2009).

Age-dependent sensitivity to the effect of ATZ on the risk distributions in this study was slight, which likely reflects slight differences in the daily volume of water consumed relative to body mass for the 2 age groups assessed here. Other age groups and males were not assessed because the toxicological endpoint (LH surge suppression) is specific for sexually mature females. However, the PODs based on developmental (Scialli *et al.*, 2014) or reproductive toxicity (DeSesso *et al.*, 2014) endpoints are 5- to 10-fold greater than those based on LH surge suppression. Therefore, the MOE results based on the LH POD are conservative.

The analysis of the sensitivity of simulated MOEs to variation in PBPK model parameters showed that the rate of clearance of DACT into urine was the predominant driver of the calculated MOE ($r^2 = 0.99$). Based on a worst-case analysis of 4-day rolling average TCT AUCs for one CWS, the results indicated that the 99.9th-percentile MOE could have been overestimated (approximately 13 000 instead of 4500) or underestimated (approximately 13 000 instead of 31 000) by a factor of approximately 3. The DACT urinary clearance parameter used in the model was derived from a human study (Campbell *et al.*, 2016), where the clearance of DACT into urine was measured in 6 subjects. In the human study, the coefficient of variation (CV) in the half-life of urinary clearance of DACT was 0.18, whereas the CV used in the model parameter simulation was 0.5. Therefore, we are confident that value selected for CRLDAC in the PBPK model used for risk assessment was both accurate and precise.

The major strength of this study is that human exposure to the chlorotriazines in drinking water is based on a large and robust database from which we selected 17 vulnerable CWSs for a detailed evaluation. Uncertainty associated with the frequency of water sample collection was quantified by 2 methods (insertion of synthetic peaks between measured values or the use of Krige estimates). Water consumption data were limited and uncertainties associated with seasonal differences in intake were not assessed. However, the drinking water data used in this study (Barraj *et al.*, 2009) included data from both summer and winter months.

The PBPK model was rederived using a comprehensive set of *in vitro* metabolism data from new studies in rat and human hepatocytes, as well as from a new *in vivo* kinetic study in rats (Campbell *et al.*, 2016). Critical parameters associated with urinary clearance of the chlorotriazines were derived from a human study. However, phase 2 metabolites (eg, glutathione and cysteine conjugates, as well as mercapturates of ATZ, DEA, DIA, and DACT) found in the urine, but not in the plasma of nonhuman primates administered ^{14}C-ATZ (unpublished data), are not represented in the model, and therefore urinary biomonitoring equivalent concentrations could not be calculated for these metabolites. We expect that an independent derivation of the PBPK model, based on nonhuman primate data, will serve to validate the human model presented in Campbell *et al.* (2016) and to extend it to include a broader spectrum of metabolites found in the urine of nonhuman primates and man. Work is also underway to expand the PBPK model to include dermal and inhalation routes of entry into the body. This will allow for a more refined interpretation of human urine biomonitoring data reported in occupational exposure studies (Selman *et al.*, 2001), in studies on specific subpopulations of individuals (Chevrier *et al.*, 2011, 2014), or in nationwide surveys (CDC, 2009).

Overall, the results from this study indicate that is highly unlikely that humans will experience adverse effects resulting from exposure to ATZ and its chlorometabolites in drinking water. When exposure to TCTs in drinking water is distributed over a 24-h day, the rapid pharmacokinetic clearance of ATZ and its chlorotriazine metabolites ensures that the internal POD dose is never reached. An assessment of MOEs at the 99.9th percentile for 17 of 149 most highly vulnerable CWSs in the ATZ drinking water surveillance program indicates that the threshold for a biological effect, as defined in animal models, is typically 3–4 orders of magnitude greater than exposure.

FUNDING

This work was supported by Syngenta Crop Protection, LLC, a registrant and basic manufacturer of ATZ. All studies were conducted by laboratories independent of Syngenta.

ACKNOWLEDGMENTS

Brian Christensen and Dennis Tierney provided the Safe Drinking Water data and Andrew Merritt provided the frequent monitoring data for the 17 CWSs. Paul Hendley (Phasea, Ltd.) provided the synthetic chemographs and Wenlin Chen supplied the Krieg estimates. Tim Pastoor reviewed an early draft of this article. The authors of this review have either served as consultants to Syngenta Crop Protection, LLC (JLC, CV-F, HJC-III, MEA, and RLS), or are Syngenta employees (CBB).

SUPPLEMENTARY DATA

Supplementary data are available online at http://toxsci.oxfordjournals.org/.

REFERENCES

Barraj, L., Scrafford, C., Lantz, J., Daniels, C., and Mihlan, G. (2009). Within-day drinking water consumption patterns: Results from a drinking water consumption survey. *J. Expo. Sci. Environ. Epidemiol.* **19**, 382–395.

Boffetta, P., Adami, H. O., Berry, S. C., and Mandel, J. S. (2013). Atrazine and cancer: A review of the epidemiologic evidence. *Eur. J. Cancer Prev.* **22**, 169–180.

Breckenridge, C. B., Eldridge, J. C., Stevens, J. T., and Simpkins, J. W. (2010). *Symmetrical Triazine Herbicides: A Review of Regulatory Toxicity Endpoints*, 3rd ed., pp. 1711–1723. Academic Press, New York.

Bridges, D. C. (2008). *Chapter 13 - Benefits of Triazine Herbicides in Corn and Sorghum Production* (H. M. LeBaron, J. E. McFarland and O. C. Burnside, Eds.), pp. 163–174. Elsevier, San Diego. doi: 10.1016/B978-044451167-6.50016-7.

Campbell, J., Andersen, M. E., Hinderliter, P. M., Yi, K. D., Pastoor, T. P., Breckenridge, C. B., and Clewell, H. J., III (2016). PBPK model for atrazine and its chlorotriazine metabolites in rat and human. *Toxicol Sci.* **150**, 441–453.

CDC. (2009). Fourth National Report on Human Exposure to Environmental Chemicals. Centers for Disease Control and Prevention. Available at: http://www.cdc.gov/exposurereport/pdf/fourthreport.pdf. Accessed on February 5, 2016.

Chen, W., Whitmore, R., and Mosquin, P. (2011). *Impact of Alternative Monitoring Frequencies on Estimation of Atrazine Rolling Average Environmental Concentrations (Addendum to MRID 48470008)*. Syngenta Crop Protection, LLC, Internal Report, G030027_50533. Greensboro, NC.

Chevrier, C., Limon, G., Monfort, C., Rouget, F., Garlantezec, R., Petit, C., Durand, G., and Cordier, S. (2011). Urinary biomarkers of prenatal atrazine exposure and adverse birth outcomes in the PELAGIE Birth Cohort. *Environ. Health Perspect.* **119**, 1034–1041.

Chevrier, C., Serrano, T., Lecerf, R., Limon, G., Petit, C., Monfort, C., Hubert-Moy, L., Durand, G., and Cordier, S. (2014). Environmental determinants of the urinary concentrations of herbicides during pregnancy: The PELAGIE mother–child cohort (France). *Environ. Int.* **63**, 11–18.

Cooper, R. L., Buckalew, A., Fraites, M., Goldman, J., Laws, S., Narotsky, M., and Stoker, T. (2010). Evaluating the effect of the Chlorotriazine Herbicide Atrazine on the amplitude of the pre-ovulatory LH surge in the Long-Evans Rat. *U.S. EPA, Internal Report*, p. 18.

Cooper, R. L., Laws, S. C., Das, P. C., Narotsky, M. G., Goldman, J. M., Lee Tyrey, E., and Stoker, T. E. (2007). Atrazine and reproductive function: Mode and mechanism of action studies. *Birth Defects Res. B Dev. Reprod. Toxicol.* **80**, 98–112. 10.1002/bdrb.20110.

DeSesso, J. M., Scialli, A. R., White, T. E., and Breckenridge, C. B. (2014). Multigeneration reproduction and male developmental toxicity studies on atrazine in rats. *Birth Defects Res. B Dev. Reprod. Toxicol.* **101**, 237–253. 10.1002/bdrb.21106.

Foradori, C. D., Hinds, L. R., Hanneman, W. H., Legare, M. E., Clay, C. M., and Handa, R. J. (2009). Atrazine inhibits pulsatile luteinizing hormone release without altering pituitary sensitivity to a gonadotropin-releasing hormone receptor agonist in female Wistar rats. *Biol. Reprod.* **81**, 40–45. biolreprod.108.075713 [pii] 10.1095/biolreprod.108.075713.

Foradori, C. D., Sawhney Coder, P., Tisdel, M., Yi, K. D., Simpkins, J. W., Handa, R. J., and Breckenridge, C. B. (2014). The effect of atrazine administered by gavage or in diet on the LH surge and reproductive performance in intact female Sprague-Dawley and Long Evans rats. *Birth Defects Res. B Dev. Reprod. Toxicol.* **101**, 262–275.

Fraites, M. J., Cooper, R. L., Buckalew, A., Jayaraman, S., Mills, L., and Laws, S. C. (2009). Characterization of the hypothalamic-pituitary-adrenal axis response to atrazine and metabolites in the female rat. *Toxicol. Sci.* **112**, 88–99.

Goldman, J., Davis, L. K., Murr, A. S., and Cooper, R. L. (2013). Atrazine-induced elevation or attenuation of the LH surge in the ovariectomized, estrogen-primed female rat: Role of adrenal progesterone. *Reproduction* **146**, 305–314. 10.1530/rep-13-0011.

Goodman, M., Mandel, J. S., DeSesso, J. M., and Scialli, A. R. (2014). Atrazine and pregnancy outcomes: A systematic review of epidemiologic evidence. *Birth Defects Res. B Dev. Reprod. Toxicol.* **101**, 215–236.

ILSI Research Foundation. (2008). CARES: Cumulative and Aggregate Risk Evaluation System. Available at: http://www.ilsi.org/Research Foundation/Pages/CARES.aspx. Accessed on February 5, 2016.

Laws, S. C., Hotchkiss, M., Ferrell, J., Jayaraman, S., Mills, L., Modic, W., Tinfo, N., Fraites, M., Stoker, T., and Cooper, R. (2009). Chlorotriazine herbicides and metabolites activate an ACTH-dependent release of corticosterone in male Wistar rats. *Toxicol. Sci.* **112**, 78–87. kfp190 [pii] 10.1093/toxsci/kfp190.

McMullin, T. S., Andersen, M. E., Nagahara, A., Lund, T. D., Pak, T., Handa, R. J., and Hanneman, W. H. (2004). Evidence that atrazine and diaminochlorotriazine inhibit the estrogen/progesterone induced surge of luteinizing hormone in female Sprague-Dawley rats without changing estrogen receptor action. *Toxicol. Sci.* **79**, 278–286. 10.1093/toxsci/kfh127 kfh127 [pii].

Minnema, D. J. (2001). Comparison of the LH Surge in Female Rats Administered Atrazine, Simazine or DACT via Oral Gavage for One Month, p. 544. Covance Laboratories Inc., Vienna, VA.

Renwick, A. G., and Lazarus, N. R. (1998). Human variability and noncancer risk assessment–An analysis of the default uncertainty factor. *Regul. Toxicol. Pharmacol.* **27**, 3–20.

Sathiakumar, N., MacLennan, P. A., Mandel, J., and Delzell, E. (2011). A review of epidemiologic studies of triazine herbicides and cancer. *Crit. Rev. Toxicol.* **41**, 1–34. 10.3109/10408444.2011.554793.

Scialli, A. R., DeSesso, J. M., and Breckenridge, C. B. (2014). Developmental toxicity studies with atrazine and its major metabolites in rats and rabbits. *Birth Defects Res. B Dev. Reprod. Toxicol.* **101**, 199–214.

Selman, F., Rosenheck, L., Breckenridge, C. B., and Stevens, J. T. (2001). Comparison estimated exposure to atrazine of commercial handlers based on PHED, whole body dosimetry and urine biomonitoring. *Toxicologist.* **60**, 16–17.

Simpkins, J. W., Swenberg, J. S., Weiss, N., Brusick, D., Eldridge, J. C., Stevens, J. T., Handa, R. J., Hovey, R. C., Plant, T. M., Pastoor, T. P., *et al.* (2011). Atrazine and breast cancer: A framework assessment of the toxicological and epidemiological evidence. *Toxicol. Sci.* **123**, 441–459. 10.1093/toxsci/kfr176.

Skøien, J. O., and Blöschl, G. (2007). Spatiotemporal topological kriging of runoff time series. *Water Resour. Res.* **43**, 1–21. 10.1029/2006wr005760.

Thurman, E. M., and Scribner, E. A. (2008). A decade of measuring, monitoring, and studying the fate and transport of triazine herbicides and their degradation products in groundwater, surface water, reservoirs, and precipitation by the US geological survey In (H. M. LeBaron, J. E. McFarland

and O. C. Burnside, Eds.), *The Triazine Herbicides*, pp. 451–475. Elsevier, San Diego.

Tierney, D. P., Christensen, B. R., Dando, C., and Marut, K. M. (2008). Chapter 29 - Atrazine and Simazine Monitoring Data in Community Water Systems in the United States during 1993 to 2000 (H. M. LeBaron, J. E. McFarland and O. C. Burnside, Eds.), pp. 439–449. Elsevier, San Diego. doi: 10.1016/B978-044451167-6.50032-5.

USDA. (2000). *CSFII Data Set and Documentation: The 1994–96, 1998 Continuing Surveys of Food Intakes by Individuals*. Food Surveys Research Group, Beltsville Human Nutrition Research Center, Agricultural Research Service, United States Department of Agriculture, Beltsville, MD.

USEPA. (2002). *The Grouping of a Series of Triazine Pesticides Based on a Common Mechanism of Toxicity*. United States Environmental Protection Agency, Office of Pesticide Programs, Health Effects Division, Washington, DC. Available at: http://www.regulations.gov/#!documentDetail;D=EPA-HQ-OPP-2005-0481-0011. Accessed on February 2, 2016.

USEPA. (2004). *Memorandum of Agreement Between the U. S. Environmental Protection Agency and Agan Chemical Manufacturing, Dow AgroSciences, Drexel Chemical, Oxon Italia S.P.A., and Syngenta Crop Protection Concerning the Registration of Pesticide Products Containing Atrazine*, p. 36. United States Environmental Protection Agency, Washington, DC.

USEPA. (2006). Special review branch, special review and registration division (7508P). *Atrazine: Finalization of Interim Reregistration Eligibility Decision and Completion of Tolerance Reassessment and Reregistration Eligibility Process*, p. 324. Office of Pesticide Programs, United States Environmental Protection Agency, Washington, DC.

USEPA. (2011a). *Re-evaluation of Human Health Effects of Atrazine: Review of Non-Cancer Effects, Drinking Water Monitoring Frequency, and Cancer Epidemiology, July 26–28, 2011, FIFRA Scientific Advisory Panel Meeting*, p. 114. FIFRA Scientific Advisory Panel, Office of Science Coordination and Policy, United States Environmental Protection Agency, Arlington, VA.

USEPA. (2011b). *Volume 1, Tables 7-4 to 7-7. In Exposure Factors Handbook: 2011 Edition*, p. 418–447. National Center for Environmental Assessment, Office of Research and Development, United States Environmental Protection Agency, Washington, DC.

USEPA. (2013). Atrazine, Propazine, and Simazine. Human Health Risk Scoping Document in Support of Registration Review, pp. 29. Risk Assessment Branch V (RAB V), Health Effects Divison (HED) (7509P), Office of Pesticide Programs, United States Environmental Protection Agency. PC Code: 080803, 080808, 080807; DP Barcode: D407489. Washington, DC.

WHO. (2005). Chemical-specific adjustment factors for interspecies differences and human variability: guidance document for use of data in dose/concentration-response assessment. World Health Organization, Geneva. Available at: http://www.inchem.org/documents/harmproj/harmproj/harmproj2.pdf. Accessed on February 5, 2016.

WHO. (2010). *Atrazine and Its Metabolites in Drinking-water: Background document for development of WHO Guidelines for Drinking-water Quality*, p. 15. WHO Document Production Services, Geneva.